J Mater Sci (2009) 44:3010–3013
DOI 10.1007/s10853-009-3431-x

LETTER

Bulk modulus of silicon carbide nanowires and nanosize grains

Ryan M. Rich · Svitlana Stelmakh · Jaromir Patyk · Monika Wieligor · T. W. Zerda · Quanzhong Guo

Received: 7 January 2009 / Accepted: 20 March 2009 / Published online: 5 April 2009

The growing interest in nanostructures stems from their unique physical and chemical properties that differ from properties of bulk materials of the same composition. Silicon carbide (SiC) nanoparticles are of particular interest, because of their high hardness, high melting temperature, excellent resistance to heat, and distinctive electronic and optical properties [1, 2]. Previously it has been noted that nanosize materials exhibit increased hardness, and attempts to utilize that property have lead to new applications, including the incorporation of nanosize materials in composites [3].

High pressure investigations of structure and properties of nanosize materials are rare. For the most part, researchers have focused their study of size related effects on phase transitions, such as in CuS_2 [4], AlN [5], ZnS [6], CdS [7], Si [8]. Size effects on bulk modulus have been less often investigated, and, to the best of our knowledge, bulk moduli for nanosize grains have been determined only for diamond [9], Ni [10], and Si [5]. Recently Si [1], SiC [1, 11, 12], GaN [1], and SiO_2 [13] nanowires have been produced in large quantities, and their physical properties have been investigated. Compressibility data for these nanowires are scarce, and the goal of this study is to provide such information on SiC nanowires for comparison with data on nanosize powders.

Silicon carbide nanowires were sintered from silicon powder of average grain size 30 nm and carbon nanotubes of average diameter between 15 and 30 nm and length ranging from 200 nm to 1.5 cm. Carbon nanotubes were purchased from Nanostructured and Amorphous Materials, Inc. and silicon from Sigma-Aldrich Co. The precursors were not mixed but placed inside a quartz tube at two separate locations. After the tube had been evacuated to a pressure less than 1 millitorr, temperature was raised to 1,200 °C. Following 1 h of sintering, temperature was quickly reduced, and a small amount of SiC nanowires was found mixed with carbon nanotubes. The carbon nanotubes were removed by heating the mixture in air at 700 °C for 2 h. Subsequent to the heat treatment, X-ray diffraction patterns showed only reflections due to SiC and none due to carbon nanotubes. Raman microanalysis also showed peaks due to SiC and none due to organized carbon or amorphous carbon.

TEM images of SiC nanowires after the heat treatment were obtained using JEOL 2100. Energy dispersive X-ray analysis (EDX) was performed using a system manufactured by EDAX.

Pressure was applied using a diamond anvil cell. The powder samples were loaded into a preindented inconel gasket along with pure gold which acted as a pressure calibrator. The pressure was calculated by determining the location of the gold (111) reflection and comparing it to data collected by Anderson et al. [14]. A mixture of methanol, ethanol, and water (16:3:1) was added as a pressure medium, and the sample was squeezed between the two diamond anvils by four manually operated screws.

High pressure XRD measurements were conducted on beamline X17B3 at the National Synchrotron Light Source in Brookhaven, New York. This beamline utilized a digital pinhole-camera apparatus with radiation measuring

---

R. M. Rich · S. Stelmakh · J. Patyk · M. Wieligor ·
T. W. Zerda (✉)
Department of Physics and Astronomy, TCU, Box 298840,
Fort Worth, TX 76129, USA
e-mail: t.zerda@tcu.edu

Q. Guo
Brookhaven National Laboratory, 75 Brookhaven Avenue,
Bldg. 725B, Upton, NY 11973-5000, USA

0.404067 Å in wavelength. The recorded images were integrated using the program Fit2D [15], producing the usual diffractogram. A sum of Voigt functions was fitted to each image with the program Fityk [16].

TEM images indicated the presence of nanosize wires with smooth surfaces and abundant stacking faults, as seen in Fig. 1. The diameters of the nanowires were measured, and they followed the log-normal distribution with the maximum at about 30 nm, see Fig. 2. From high resolution TEM images, inset in Fig. 1, it is evident that the interior was crystalline with average distance of 2.5260 Å between (111) crystallographic planes, as determined by XRD. EDX analysis showed that the interiors of the nanowires were pure silicon carbide, while the amorphous layer was mainly SiC with some oxygen present. Si–O bonds were detected by FTIR analysis, and they were probably formed during the removal of excess carbon nanotubes by post production heating.

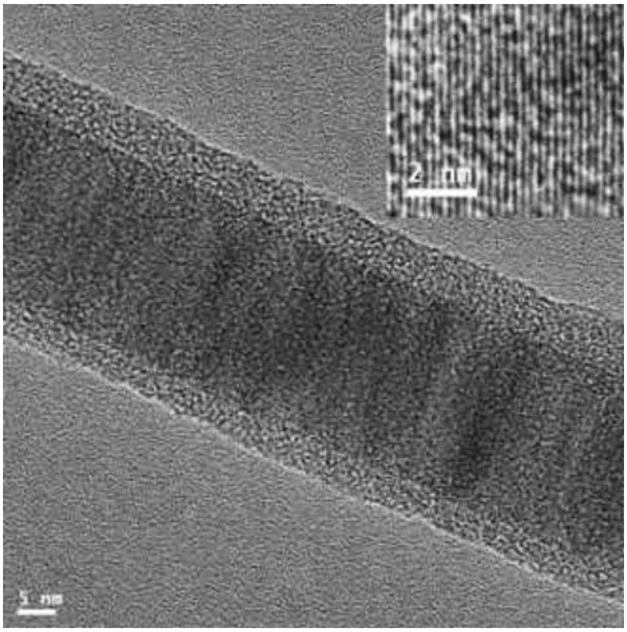

Fig. 1 HRTEM image of a silicon carbide nanowire. The crystalline core is surrounded by an approximately 5 nm layer of amorphous material. The inset shows a magnified image of the nanowire interior with regularly spaced crystalline structure

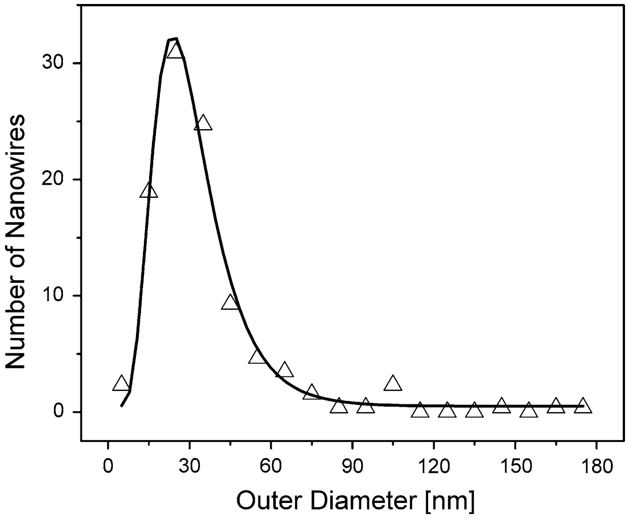

Fig. 2 Log-normal distribution of SiC nanowire diameters

Prior to high pressure measurements, XRD measurements were performed on all specimens using a Phillips diffractometer with copper $K_{\alpha1}$ excitation. Broadening of the (111) reflection for nanosize samples, depicted in Fig. 3, is directly related to reduced crystallite sizes. Due to physical limitations of the high pressure anvil cell, the diffractograms were limited to angles less than 20°. The short wavelength of incident radiation allowed us to record two reflections due to gold and three peaks due to SiC (111), (200), and (220) reflections. To find their positions, experimental contours were fitted to a sum of seven Voigt functions: five for SiC and two for gold. Peak positions enabled calculations of the lattice constant, and lattice constant calculations performed on gold allowed the determination of pressure within the diamond anvil cell. Figure 4 illustrates pressure induced shifts of the (111) reflection of SiC. Lattice parameter calculations carried out on SiC diffraction data were later used to determine the volume of the SiC lattice cell. The bulk modulus was calculated by fitting experimental data to the Birch–Murnaghan equation

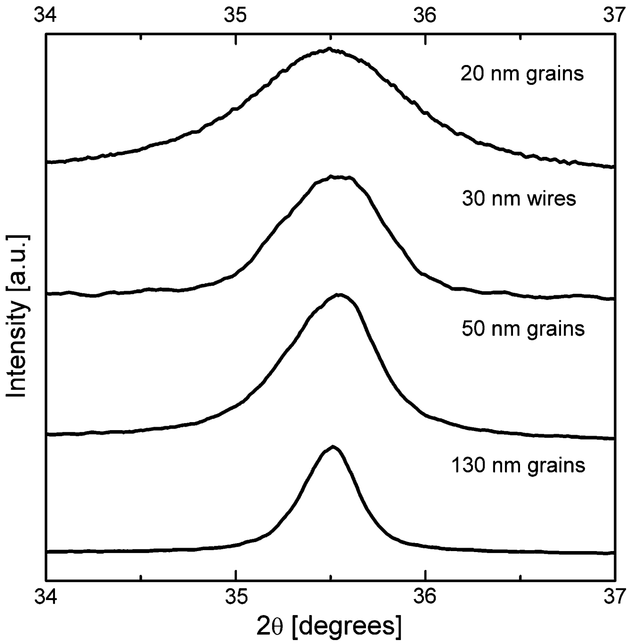

Fig. 3 Size related broadening of the (111) reflection of SiC

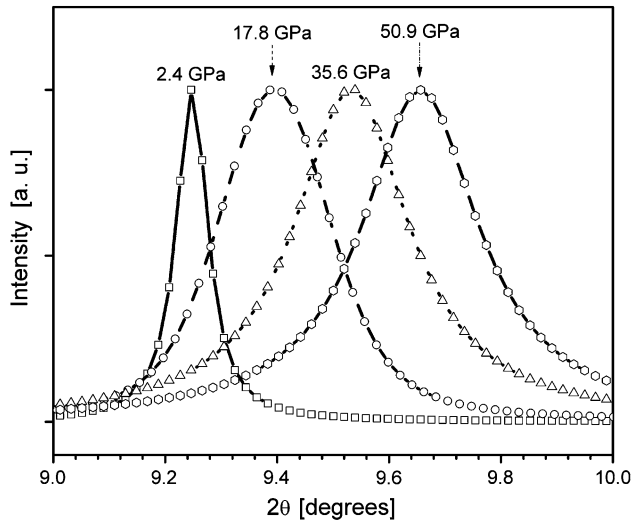

Fig. 4 Pressure induced shift of the (111) reflection for the nanowires. To guide the eye, experimental points recorded at different pressures are connected by lines

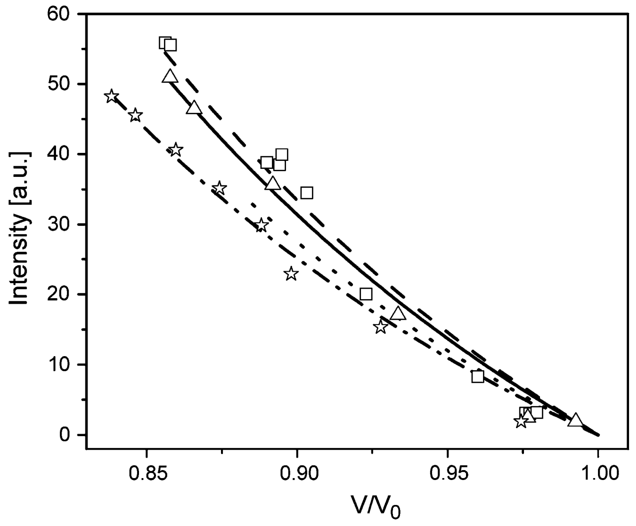

Fig. 5 Experimental data points for the 130 nm SiC powder (*stars*), the 20 nm powder (*squares*) and the 30 nm nanowires (*triangles*). Data points corresponding to 50 nm powder were omitted for clarity. The solid line represents the best fitting of Eq. 1 to the data obtained for the nanowires, the broken line—the 20 nm SiC powder, the dotted line—the 50 nm powder, and the dash-dotted line for the 130 nm SiC powder

$$P=\frac{3}{2}K\left[\left(\frac{V}{V_0}\right)^{-\frac{7}{3}}-\left(\frac{V}{V_0}\right)^{-\frac{5}{3}}\right]\left\{1+\frac{3}{4}(K'-4)\left[\left(\frac{V}{V_0}\right)^{-\frac{2}{3}}-1\right]\right\} \tag{1}$$

where V/V_0 is the reduced volume, P is the applied pressure, and K and K' are the fitting parameters, the bulk modulus and its derivative, respectively. Initially we considered K' an independent variable but the improvements in the fitting routine, judged by the χ^2, values were insignificant. Following previous calculations, we assumed that $K' = 4$ [17]. The results of the fittings for all specimens are shown in Fig. 5. Some of the experimental data points shown in that figure are averages of two independent measurements. For clarity reasons experimental points for the 50 nm powder are not shown. Often, these points overlapped with the values obtained for the 130 nm sample.

The bulk moduli of the 50 and 130 nm samples agree with available literature data for bulk SiC [18]. The 20 nm grains showed a significantly higher bulk modulus of about 260 GPa. The nanowires showed a bulk modulus between that of the 20 and 50 nm grains.

The elevated bulk modulus of 20 nm grains is explained by the core–shell model developed by Palosz et al. [19]. This model assumes that the individual SiC grain contains two distinct atomic arrangements: the core and the shell. In the core, the majority of the Si and C atoms are arranged in a manner consistent with bulk SiC. In our case, both the core and the shell consist of 3C SiC. It is important that the reader not confuse the shell with the amorphous layer seen in Fig. 1. The core atoms exhibit all the properties associated with the bulk material, such as bulk modulus and lattice parameter. The shell atoms, on the other hand, possess unique qualities due to the fact that their interatomic distances may differ when compared to bulk/core atoms. With nanosized materials, a much larger percentage of the constituent atoms belong to the shell, and this may lead to unique properties dependent upon particulate size.

Previous studies show that SiC particles 20 nm or smaller have shell structures with decreased interatomic distances [20]. In other words, the shell atoms are compressed. The effects of this phenomenon are seen in this study, as the 20 nm grains exhibited a high bulk modulus. It is logical that these particles better resist compression, because the shell atoms are initially compressed and therefore resist further changes. As seen in Table 1, the 50 and 130 nm particles have bulk moduli very similar to that of bulk SiC [18]. Palosz et al. [19] showed that the shell atoms belonging to particles of 80 nm or larger in size have similar interatomic distances as the core atoms. The shell of large crystals is also compressed but to a lesser extent. In

Table 1 Bulk moduli from X-ray diffraction experiment

Sample	K (GPa)
Bulk SiC [18]	203 ± 6
130 nm grains	193 ± 6
50 nm grains	198 ± 12
Nanowires (30 nm)	241 ± 17
20 nm grains	260 ± 39

addition, the relative volume of the shell is much smaller than that of the core, and therefore, the high-pressure properties of large size crystals are similar to those of the bulk material.

It is assumed that the amorphous layer has little effect on the compressibility of the core–shell structure of the nanowires.

In summary, high-pressure X-ray diffraction of SiC particles in three sizes were conducted: 20, 50, and 130 nm. The bulk moduli of the two largest sizes were consistent with bulk material, while the bulk modulus of 20 nm grains was greatly elevated. This is consistent with the core–shell model, in which studies have shown that grains 20 nm or smaller possess compressed shell atoms. Results for the 30 nm SiC nanowires indicate that their bulk moduli are smaller than those for the 20 nm grains but larger than for the 50 nm grains. At this stage of this research it is impossible to separate the size effect from the effect of the morphology.

Acknowledgements This study was supported by a grant NSF DMR 0502136. Svitlana Stelmakh acknowledges the Polish Ministry of Education and Science, grant 3 T08A 020 29, for the partial support of this research. Use of the National Synchrotron Light Source, Brookhaven National Laboratory, was supported by the U.S. Department of Energy, Office of Science, Office of Basic Energy Sciences, under Contract No. DE-AC02-98CH10886.

References

1. Bhustan B (ed) (2007) Springer handbook of nanotechnology. Springer, New York
2. Shackelford JF, Alexander W, Park JS (eds) (1994) CRC materials science and engineering handbook. CRC Press, Boca Raton
3. Ekimov EA, Gavriliuk AG, Palosz B, Gierlotka S, Dluzewski P, Tatianin E, Kluev Y, Naletov AM, Presz A (2000) Appl Phys Lett 77:954
4. Wang S, Guo L, Wen X, Yang S, Zhao J, Liu J, Wu Z (2002) Mater Chem Phys 75:32
5. Shen LH, Li XF, Ma YM, Yang KF, Lei WW, Cui QL, Zou GT (2006) Appl Phys Lett 89:141903
6. Wang Z, Daemen LL, Zhao Y, Zha C, Downs RT, Wang X, Wang Z, Hempley R (2005) Nat Mater 4:922
7. Fan HM, Ni ZH, Feng YP, Fan XF, Shen ZX, Zou BS (2008) J Raman Spectrosc 38:1112
8. Wang Y, Zhang J, Wu J, Coffer J, Lin Z, Sinogeikin S, Yang W, Zhao Y (2008) Nano Lett 8:2891
9. Pantea C, Zhang J, Qian J, Zhao Y, Migliori A, Grzanka E, Palosz B, Wang Y, Zerda TW, Liu, H, Ding Y, Stephens PW, Botez CE (2006) In: Technical proceedings of the 2006 nanotechnology conference and trade show, vol 1, p 823
10. Zhang J, Zhao Y, Palosz B (2007) Appl Phys Lett 90:043112
11. Li F, Wen G (2007) J Mater Sci 42:4125. doi:10.1007/s10853-007-1682-y
12. Wallis KL, Wieligor M, Zerda TW, Stelmakh S, Gierlotka S, Palosz B (2008) J Nanosci Nanotechnol 8:3504
13. Liang CH, Zhang LD, Meng GW, Wang YW, Chu ZQ (2000) J Non-Cryst Solids 277:63
14. Anderson OL, Isaak DG, Yamamoto S (1989) J Appl Phys 65:4
15. Hammersley A (1994) Computer software. Fit2D. Grenoble
16. Wojdyr M (2004) Computer software, *Fityk*, Unipress. http://www.unipress.waw.pl/fityk
17. Liu H, Hu J, Shu J, Häusermann D, Mao H (2004) Appl Phys Lett 85:11
18. NIST property data summaries for sintered silicon carbide (SiC). NIST structural ceramics database, SRD database number 30. National Institute of Standards and Technology. http://www.ceramics.nist.gov/srd/summary/scdscs.htm
19. Palosz B, Stelmakh S, Grzanka E, Gierlotka S, Palosz W (2007) Z Kristallogr 222:580
20. Palosz B, Stel'makh S, Grzanka E, Gierlotka S, Pielaszek R, Bismayer U, Werner S, Palosz W (2004) J Phys Condens Matter 16:S353